# Initial oxidation kinetics of Cu(100), (110), and (111) thin films investigated by in situ ultra-high-vacuum transmission electron microscopy

Guangwen Zhou[a] and Judith C. Yang[b]
*Department of Materials Science and Engineering, University of Pittsburgh, Pittsburgh, Pennsylvania 15261*

(Received 4 January 2005; accepted 18 April 2005)

The initial oxidation stages of Cu(100), (110), and (111) surfaces have been investigated by using in situ ultra-high-vacuum transmission electron microscopy (TEM) techniques to visualize the nucleation and growth of oxide islands. The kinetic data on the nucleation and growth of oxide islands shows a highly enhanced initial oxidation rate on the Cu(110) surface as compared with Cu(100), and it is found that the dominant mechanism for the nucleation and growth is oxygen surface diffusion in the oxidation of Cu(100) and (110). The oxidation of Cu(111) shows a dramatically different behavior from that of the other two orientations, and the in situ TEM observation reveals that the initial stages of Cu(111) oxidation are dominated by the nucleation of oxide islands at temperatures lower than 550 °C, and are dominated by two-dimensional oxide growth at temperatures higher than 550 °C. This dependence of the oxidation behavior on the crystal orientation and temperature is attributed to the structures of the oxygen-chemisorbed layer, oxygen surface diffusion, surface energy, and the interfacial strain energy.

## I. INTRODUCTION

The classic theories of oxidation, such as the theory of Wagner[1] and the Cabrera-Mott model,[2] have proved to be highly successful in predicting the oxidation behavior of metals, but these models are focused on the growth of an oxide layer and assume uniform film growth controlled by the transport of ionic species through the continuous oxide film. Due to the development of well-controlled experiments and the increased experimental capabilities in terms of resolution and cleanliness, it is known now that the early stages of metal oxidation typically involve the nucleation and initial growth of metal oxide islands, rather than the formation and thickening of a continuous film,[3–7] which represents a critical departure from previously held assumptions in the classic theories regarding metal oxidation.[1,2]

An ideal technique for probing the initial oxide formation is in situ transmission electron microscopy (TEM). Most TEM studies of oxide scales have relied on the examination of oxide films after they have been stripped from the metal. Such a technique has the disadvantage of changing the relative position of the oxide film on the substrate and prohibits the accurate determination of the orientation relationships between the oxide and the base metal. Furthermore, one cannot study the initial stages of the oxide scale since one cannot strip off discontinuous layers. Previous investigators have recognized the importance of graphene oxidation techniques and have studied the initial stages of oxidation by in situ techniques, including TEM, but obtaining an atomically clean surface was impossible with previously available experimental techniques.[8] Impurities play a dramatic role in oxidation kinetics.[9] The surface impurities must be controlled to gain quantitative and fundamental information about oxidation. Some previous in situ TEM investigations involved a side chamber for oxidation processing, then the samples were transferred to the transmission electron microscope column for observation. The nucleation, initial growth, and structure changes of the oxide were not followed in real time. Therefore, the nucleation and growth of oxide islands were interrupted during oxidation for the TEM observation, and some important information was missing that is critical to understanding the oxidation mechanism. In situ ultra-high-vacuum (UHV) TEM combines the correct range in

[a] Address all correspondence to this author.
Present address: Materials Science Division, Argonne National Laboratory, Argonne, IL 60439.
e-mail: gzhou@anl.gov
[b] This author was an editor of this focus issue during the review and decision stage. For the *JMR* policy on review and publication of manuscripts authored by editors, please refer to http://www.mrs.org/publications/jmr/policy.html.
DOI: 10.1557/JMR.2005.0239

 

spatial resolution for bridging the gap between nucleation and the initial growth of the oxide with the provision of the UHV environment that is necessary for atomically clean surfaces. The advantages of in situ UHV TEM experiments include visualization of the oxidation processes in real time and information on buried interfaces. The microscope provides dynamic information from nucleation to the initial growth and coalescence of the oxide islands at the nanometer scale. One can now see structural changes under controlled surface conditions. This experimental tool provides unique and critical data on these gas surface reactions in the wide pressure and temperature range that is needed for a fundamental understanding of the atomistic kinetics.

By using in situ UHV TEM, Yang and colleagues[6,10] investigated the kinetics in the initial stages of Cu(100) oxidation and revealed that oxygen surface diffusion is the dominant mechanism for oxide formation during the initial oxidation in a dry oxygen atmosphere. This study was later extended to the case of the Cu(110) surface.[11] In this review article, we first compare the kinetics in the initial oxidation stages of Cu(100) and Cu(110) surfaces, and then present some interesting new results from the oxidation of the Cu(111) surface. Our results indicate that the oxidation of Cu(100) and (110) can be described by the oxygen surface diffusion model. But the Cu(111) surfaces show a dramatically different oxidation behavior from the other two orientations. The oxidation is dominated by the nucleation of oxide islands at low temperatures, and nearly two-dimensional (2D) oxide growth dominates at high temperatures. This investigation demonstrates that the starting surface structure has a dramatic effect on the initial oxide formation, which may have a further effect on the long-term oxidation rate. Before presenting the results from in situ UHV TEM experiments, we first briefly introduce the oxygen surface diffusion model that was developed to describe the initial oxidation stages.[5,6]

## II. OXYGEN SURFACE DIFFUSION MODEL

### A. Nucleation

During the nucleation stage, oxygen impinges upon the substrate, diffuses across the surface and may be lost to re-evaporation, forms new nuclei, or incorporates into an existing $Cu_2O$ nucleus. Regardless of the details of the intermediate steps, the density of these stable nuclei is expected to increase with time, and the probability of an oxide nucleation event is proportional to the fraction of the available surface area

$$dN = k(1 - L_d^2)dt \quad , \tag{1}$$

where $N$ is the number density of the nuclei, $t$ is the time, $L_d^2$ is the area of the zone of oxygen capture around each $Cu_2O$ island, and $k$ is a proportionality of constant, which depends on the probability for Cu and O to form $Cu_2O$. Using the boundary condition that at $t = 0$, $N = 0$, and solving Eq. (1), we obtain

$$N = \frac{1}{L_d^2}(1 - e^{kL_d^2 t}) \quad . \tag{2}$$

One consequence of oxygen surface diffusion being the mechanism for nucleation is that there is a saturation level, $N_s = 1/L_d^2$, and then decreases as the discrete nuclei grow into larger islands and coalesce. This is due to the existence of an active zone of oxygen capture around each oxide island long before the islands impinge on each other, where the radius of this capture zone is dependent on the surface processes. Because of the higher mobility of oxygen at higher temperatures, the attachment to an existing island is more favorable than the nucleation of a new nucleus. Hence, it is reasonable to expect many small islands to form at low temperatures, whereas for high temperatures a lower island density, but a larger island size, is expected. The saturation island density dependence on temperature follows an Arrhenius relationship

$$N_S \sim e^{-E_a/kT} \quad , \tag{3}$$

where $k$ is the Boltzmann constant, $T$ is the oxidation temperature. This activation energy, $E_a$, for the nucleation of oxide islands depends on the energies of nucleation, absorption, and/or desorption, and oxygen surface diffusion.[12] By measuring the saturation island density at different temperatures, then the activation energy, $E_a$, for this surface-limited nucleation process can be determined.

### B. Growth

As discussed above, there exists an active zone of oxygen capture around each oxide island, and oxygen that lands inside this zone may diffuse to the $Cu_2O$ island, leading to the growth of the island. When the zone of oxygen capture of each island starts to impinge on each other zone, then no further nucleation can occur and an island saturation density has been reached. Orr,[4] followed by Holloway and Hudson,[3] had developed an oxidation model based on the assumption that oxygen surface diffusion plays a major role in the initial growth of the metal oxide. They assumed that the oxide islands grow on the metal surface (i.e., 2D), and the dominant transport mechanism for the island growth is the oxygen surface diffusion and impingement on the perimeter of an oxide island. Following the derivation of Orr,[4] oxygen surface diffusion to the perimeter of an oxide island creates a growth rate[3]

$$\frac{dP(t)}{dt} = 2\pi r K_s f_s \quad , \tag{4}$$

where $P(t)$ is the number of oxygen atoms in $Cu_2O$ island at time $t$, $r$ is the radius of an island, $K_s$ is the sticking coefficient of oxygen to the $Cu_2O$ island perimeter, and $f_S$ is the diffusive flux of oxygen. For 2D lateral growth of a disk-shaped island, with thickness $a$, then by solving the above differential equation, the increase of the island area with respect to time follows $A(t) \sim t$.[2,3] Following a similar analysis for three-dimensional (3D) growth of an island, the area $A$, of the oxide island, is

$$A(t) = \pi \Omega K_s f_s (t - t_0) \quad , \tag{5}$$

where $\Omega$ is the volume occupied by one O atom in $Cu_2O$. Therefore, the increase of the island area $A$ has $t^2$ dependence on the oxidation time for 2D growth, and $t$ dependence for 3D growth.

## III. EXPERIMENT

The microscope used in this work was a modified JEOL 200CX (Tokyo, Japan).[13] A UHV chamber was attached to the middle of the column, where the base pressure was ~$10^{-8}$ Torr without the use of the cryoshroud. The cryoshroud inside the microscope column can reduce the base pressure to approximately $10^{-9}$ Torr when filled with liquid helium. The microscope was operated at 100 KeV to minimize irradiation effects. A leak valve attached to the column of the microscope permits the introduction of gases directly into the microscope. The specially designed sample holder allows for resistive heating at temperatures between room temperature and 1000 °C. Single crystals of Cu(100), (110), and (111) films were grown, respectively, on (100), (110), and (111) NaCl substrates in an UHV e-beam evaporator system. Films 700 ~ 800 Å thick were examined so that the films were thin enough to be examined by TEM. The copper film was removed from the substrate by floatation in deionized water, were washed, and were mounted on a specially prepared Si mount. The native Cu oxide can be removed inside the TEM by annealing the Cu films in a vacuum at ~750 °C[14] or in methanol vapor at a pressure of $5 \times 10^{-5}$ Torr but a lower temperature of 350 °C, which reduces the copper oxides to copper.[15] Oxygen gas (99.999% purity) can be admitted into the column of the microscope through the leak valve at a partial pressure between $5 \times 10^{-5}$ Torr and 760 $t$.

## IV. RESULTS

### A. Nucleation of oxide islands

The in situ observation of the island nucleation events as a function of time provides significant insights into the nucleation kinetics. Figure 1 is a sequence of the dark-field (DF) TEM images taken from $Cu_2O(110)$ reflection, showing the nucleation event of $Cu_2O$ islands in the oxidation of Cu(100) and (110) surfaces at 350 °C and an oxygen pressure of $5 \times 10^{-4}$ Torr. After the introduction of oxygen gas, no oxide islands appear within the first couple of minutes. The oxide islands are then observed to nucleate rapidly, followed by the island growth. After some time of oxidation, the islands reached the saturation density of the nuclei, and the saturation time is ~22 min

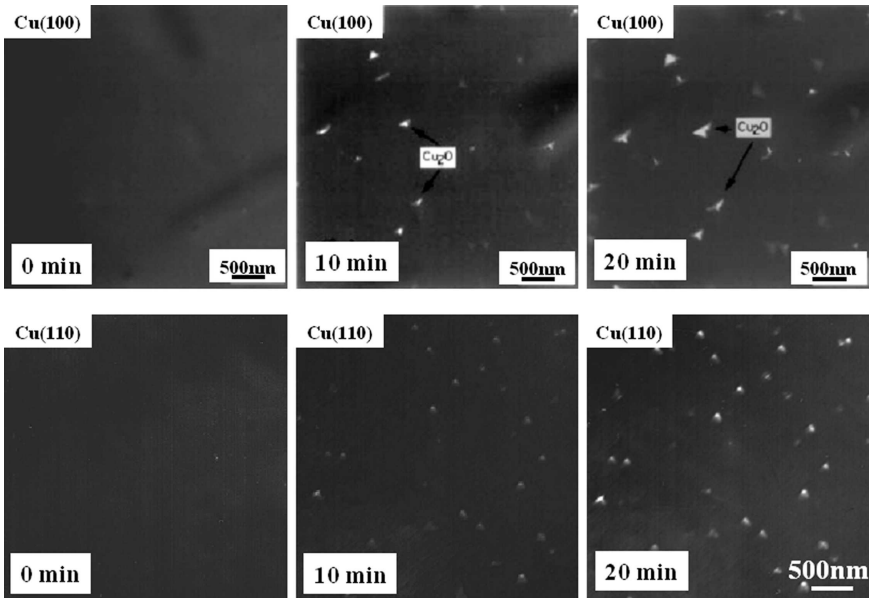


FIG. 1. $Cu_2O$ DF images taken at 0, 10, and 20 min after $O_2$ was introduced into the TEM in the oxidation of Cu(100) and Cu(110) thin films at a pressure of $5 \times 10^{-4}$ Torr at a temperature of 350 °C.

for Cu(100), and ~17 min for Cu(110). The selected-area electron diffraction patterns of the $Cu_2O$ island and underlying substrate reveal that the oxide islands are crystallographically aligned with the underlying Cu film [i.e., (001)Cu//(001)$Cu_2O$ and (010)Cu //(010)$Cu_2O$ for Cu(100), and $(1\bar{1}0)$Cu//$(1\bar{1}0)Cu_2O$ and (001)Cu//(001)$Cu_2O$ for Cu(110)].

To measure quantitatively the number density and cross-sectional area of the oxide islands, the negatives were digitized with a Leafscan 45 (Leaf Systems, Inc., MA). The software packages Digital Micrograph (Gatan Inc., Pleasanton, CA) and NIH Image were used to determine the number density and the cross-section area of the islands as a function of oxidation time. Figure 2 shows the measured density of the oxide islands with respect to the oxidation time and theoretical fit to Eq. (2). A good match is noted where the fit parameters are given in Table I.

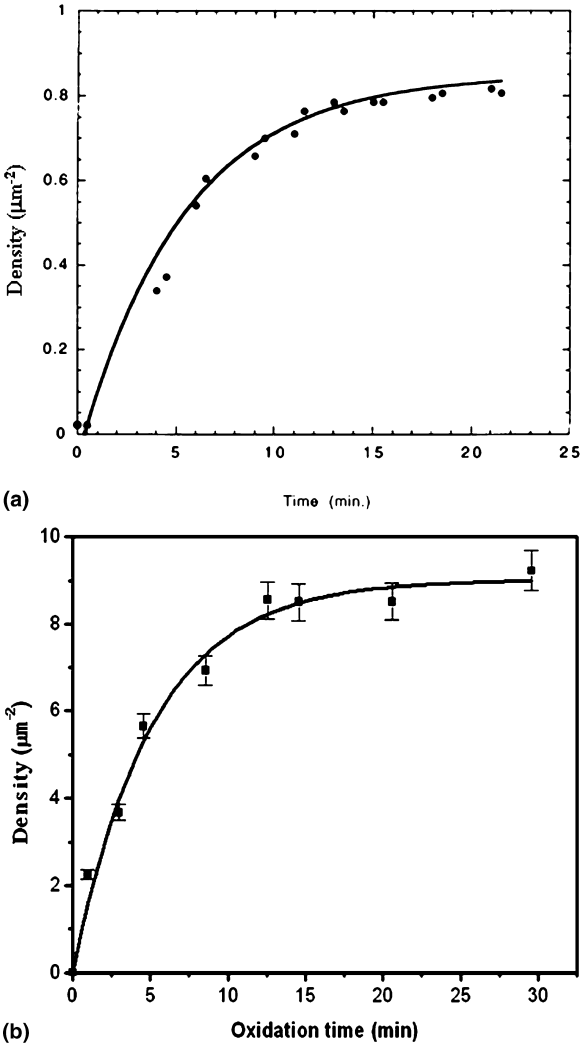


FIG. 2. $Cu_2O$ island density as a function of oxidation time at 350 °C and an oxygen pressure of $5 \times 10^{-4}$ Torr: (a) Cu(100) surface; (b) Cu(110) surface. The solid lines correspond to the theoretical fitting by using Eq. (2).

As previously mentioned, the saturation density of oxide islands follows an Arrhenius dependence on oxidation temperature. We measured the saturation density of the nuclei as a function of oxidation temperature, from ~300 °C to ~450 °C, at a constant oxygen pressure of $5 \times 10^{-4}$ Torr. Figure 3 shows the saturation density of nuclei versus inverse temperature in the oxidation of Cu(100) and (110) surfaces, where the activation energy $E_a$ for the nucleation of oxide islands, which is equal to the absolute value of the slope, is determined and given in Table I. The determined nucleation activation energy $E_a$ is model-dependent, where it could depend on the energies of nucleation, oxygen surface diffusion, absorption, and/or desorption.

### B. Growth of oxide islands

The evolution of the island area during island growth is recorded in situ. Figure 4(a) shows the TEM sequence images of the same area of the Cu(100) thin film after oxygen was admitted into the microscope at a pressure of $5 \times 10^{-4}$ Torr at a temperature of 350 °C. Figure 4(b) is a sequence of images focusing on the growth of individual islands in the oxidation of Cu(110) at 450 °C and an oxygen pressure of $5 \times 10^{-4}$ Torr. The weaker contrast features in the images could be related to the terraces on the surface, as confirmed by ex situ atomic force microscopy AFM.[16] After the nucleation of the oxide islands, it is noted that the saturation island density is reached and no new nucleation is observed in the later growth. A saturation number density of the oxide islands is observed on both orientations of the copper films, which is indicative of a surface-limited growth phenomenon.

The best power law fit to the island growth in the oxidation of the Cu(100) surface [Fig. 3(a)] is 1.3, which is slightly higher than $t$, the predicted power law dependence for 3D growth by oxygen surface diffusion. To account for the slight deviation from the linear growth, Yang et al.[5] have considered the direct impingement or bulk diffusion of oxygen that contributes to the island growth and have obtained a good fit to the experimental data, as shown in Fig. 5(a) where the solid line corresponds to the fitting by oxygen surface diffusion plus oxygen direct impingement. The experimental data of the oxide area as a function of oxidation time in the oxidation of Cu(110) are shown in Fig. 5(b). It is noted that the island area increases linearly with oxidation time, which is consistent with the 3D oxide growth limited by the surface diffusion of oxygen to the island perimeter. The solid line in Fig. 5(b) corresponds to the fitting by using Eq. (4). This linear growth of the island area indicates that oxygen surface diffusion is the dominant mechanism for the oxide growth, and the oxygen direct impingement and/or bulk diffusion is not important in the oxidation of Cu(110) at this temperature and oxygen pressure.

It is reasonable to expect that oxygen surface diffusion

TABLE I. Comparison of the nucleation kinetics in the oxidation of Cu(100) and Cu(110) at 350 °C and an oxygen pressure of $5 \times 10^{-4}$ Torr.

| Surface | Initial nucleation rate (k:$\mu m^{-2}/min^{-1}$) | Radius of oxygen capture zone ($L_d$:$\mu m$) | Saturation island density ($1/L_d^2$:$\mu m^{-2}$) | Island density saturation time (min) | Nucleation activation energy ($E_a$:eV) |
|---|---|---|---|---|---|
| Cu(100) | 0.17 | 1.09 | 0.83 | 22 | 1.4 ± 0.2 |
| Cu(110) | 1.743 | 0.33 | 9.01 | 17 | 1.1 ± 0.2 |

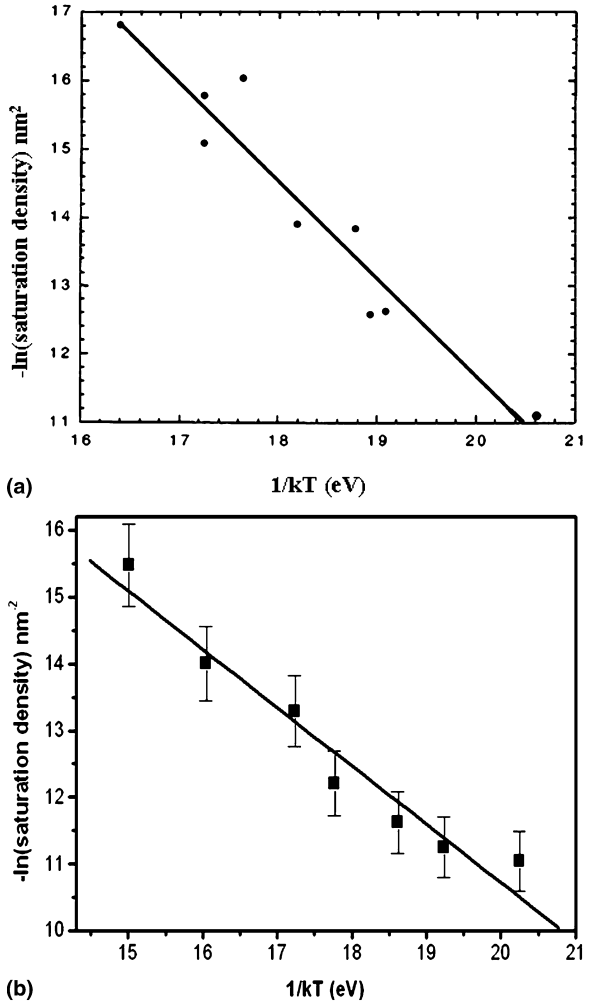


FIG. 3. The Arrhenius dependence of the saturation island density on oxidation temperature: (a) Cu(100) surface and (b) Cu(110) surface. The absolute value for the slope is the $E_a$ for the surface-limited process.

initially will dominate the oxide growth and, later, that oxygen direct impingement will contribute to the oxide growth when the islands grow larger in size, especially for the Cu film with a large coverage of the oxide islands. By considering an equal contribution of oxygen surface diffusion and direct impingement/bulk diffusion to the oxide growth, we can make an estimation of the critical area, *Ac*, of an oxide island, where we need to consider oxygen direct impingement/bulk diffusion,[17] as

$$A_c = \pi \times \left(\frac{K_1}{K_2}\right)^2 \quad , \tag{6}$$

where $K_1$ is the parameter related to the contribution of oxygen surface diffusion to the oxide island growth, and $K_2$ is the parameter related to the contribution of oxygen direct impingement to the oxide growth. According to the fit parameters obtained in the oxidation of Cu(100) at 350 °C,[5] we can know that the critical island area is ~9000 $nm^2$, which is much smaller than that in the oxidation of Cu(110), as shown in Fig. 5(b).

### C. Cu(111) oxidation

The Cu(111) surface shows a dramatically different oxidation behavior from Cu(100) and (110), and it is found that the initial stages of the Cu(111) oxidation are dominated by the nucleation of oxide islands at temperatures lower than 550 °C and by 2D oxide growth at temperatures higher than 550 °C.

Figure 6 consists of bright-field (BF) TEM sequence images showing the nucleation of oxide islands at 350 °C and an oxygen pressure of $5 \times 10^{-4}$ Torr. Compared to the oxidation of Cu(100) and (110), the nucleation rate of oxide islands on Cu(111) is much faster. Figure 6 also shows that the islands appear to show black-white contrast features, which may be related to the misfit strain in the oxide islands.

Figure 7 is the in situ observation of the nucleation and growth of oxide islands at 450 °C and an oxygen pressure of $5 \times 10^{-4}$ Torr. At the very beginning of the oxidation, the oxide islands have a random distribution. But upon further oxidation, the new oxide islands nucleate near an existing nucleus, creating clusters of oxide islands. Another intriguing feature in Fig. 7 is that the oxide islands are highly anisotropic, with the preferred elongation occurring along the [110]Cu direction. This anisotropic growth morphology may be related to a different sticking coefficient of oxygen at the island ends and sides. The island ends may have a large O-sticking coefficient that leads to the elongation of the islands, while the oxide island sides have a small O-sticking coefficient that leads to the nucleation of new islands in the area near the island sides. Figure 7 shows that the preferred sites for the nucleation of new oxide islands are in the regions near the sides of the existing islands, rather than in front of the island ends.

The oxidation of Cu(111) in the temperature range of 550–650 °C shows a very different behavior. The exposure of Cu(111) to oxygen in this temperature range results in the rapid formation of the oxide followed by fast

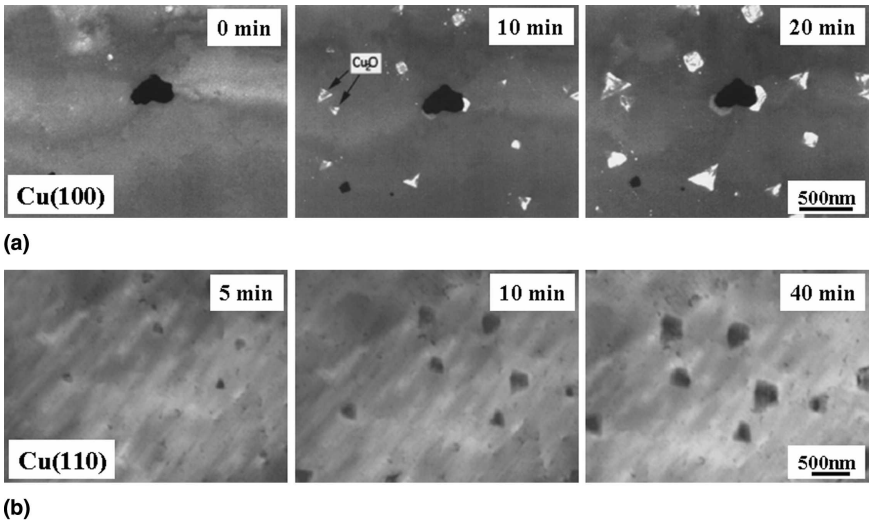


FIG. 4. (a) DF images taken from the $Cu_2O(110)$ reflection in the oxidation of Cu(100) thin film at 350 °C and an oxygen pressure of $5 \times 10^{-4}$ Torr. (b) BF images obtained in the oxidation of a Cu(110) thin film at 450 °C and an oxygen pressure of $5 \times 10^{-4}$ Torr.

lateral growth, which appears similar to the 2D development of a discontinuous oxide layer, as shown in Fig. 8. The oxide layer has an overall morphology of triangular shape with a discontinuous and disordered "cellular" structure inside the oxide layer.

The oxide formed at temperatures of 700 °C and higher has a continuous film structure and appears as 2D growth, as shown in Fig. 9, where two islands with triangular shapes are present. With the continued oxidation, coalescence occurs between these two islands. A kink forms after the coalescence, and the kink moves to the island corner along the island edge during the further growth of these two oxides. No grain boundary structure was found between the two islands, which indicative of a perfect merging of the two islands.

## V. DISCUSSION

The comparison of the initial oxidation kinetics among the Cu(100), (110), and (111) surfaces reveals that the initial oxide formation strongly depends on the crystal orientations. The kinetic data on the nucleation and growth of oxide islands indicate that Cu(110) exhibits a faster initial oxidation rate than Cu(100). The oxidation of Cu(111) shows a dramatically different behavior from Cu(100) and (110), and the initial stages of Cu(111) oxidation are dominated by the nucleation of oxide islands at temperatures lower than 550 °C, and are dominated by 2D oxide growth at temperatures higher than 550 °C.

Since the initial stages of oxidation are surface processes, it is reasonable to expect that the crystallographic orientation of the underlying metal will have a major effect on the nucleation, growth rate, and orientation of the oxide. To explain the observed dependence of the oxidation behavior on the crystallography, we consider the effects of surface structure on the kinetics and energetics of oxide formation. The nucleation and growth of oxide islands are nonequilibrium processes depending on both the energetics, such as surface energies of the system, and the kinetics, in particular the diffusion process.

### A. Effect of surface structure on the oxide formation

The general sequence of oxidation reaction on a clean metal surface is oxygen chemisorption, nucleation and growth of the oxide, and bulk oxide growth. Previous investigators have elegantly demonstrated that Cu(100) and (110) surfaces are unreconstructed and then transform into "missing-row" or "adding-row" reconstruction when exposed to oxygen.[18–20] After reconstruction, oxygen diffuses on the reconstructed surface, and nucleation occurs on the reconstructed Cu–O surface. Future arriving oxygen can either nucleate new oxide islands by reacting with copper atoms or can attach to an existing island, causing growth. Therefore, the surface diffusion coefficient of oxygen determines the outcome of the competition between nucleation and growth, and, hence, determines the number density of the stable islands. Qualitatively, a larger diffusion coefficient for oxygen should yield a lower number density of stable islands. Since the path length of oxygen surface diffusion depends on the atomic structure of the substrate plane, different nucleation behavior of $Cu_2O$ islands is therefore expected for different orientations of the Cu. The Cu(100) has a more close-packed structure and is smoother than the corrugated Cu(110) surface. Similarly, the reconstructed $(\sqrt{2} \times 2\sqrt{2})R45°$ O–Cu(100) surface has more compact oxygen chemisorption than the $(2 \times 1)$O–Cu(110) surface, which has a corrugated structure, as shown in Fig. 10. Therefore, it is expected the activation

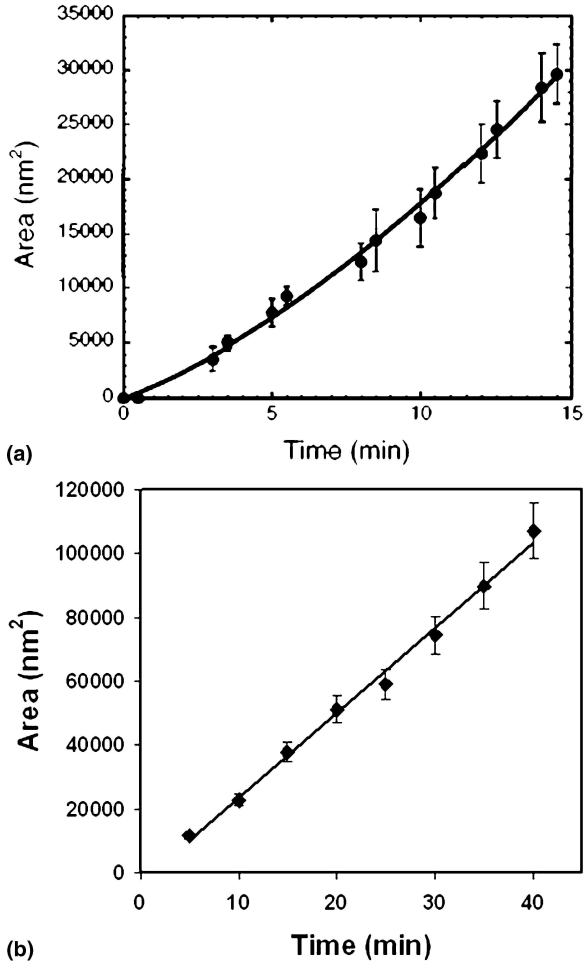


FIG. 5. (a) Comparison of the experimental data of the island area and the theoretical fitting of the oxygen surface diffusion and direct impingement/bulk diffusion for the 3D growth of $Cu_2O$ islands in the oxidation of Cu(100) thin film at 350 °C and an oxygen pressure of $5 \times 10^{-4}$ Torr. (b) Comparison of the experimental data of the island area and the theoretical fitting of the oxygen surface diffusion for the 3D growth of $Cu_2O$ islands in the oxidation of Cu(110) thin film at 450 °C and an oxygen pressure of $5 \times 10^{-4}$ Torr.

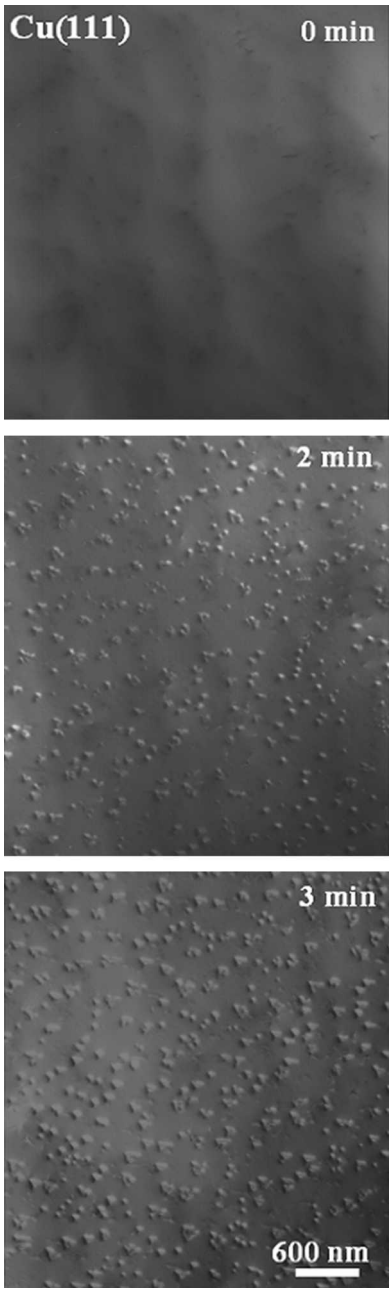


FIG. 6. In situ BF TEM images taken as a function of oxidation time at a constant oxygen partial pressure of $5 \times 10^{-4}$ Torr and a temperature of 350 °C.

barrier of the surface diffusion of the dissociated oxygen be higher on the Cu(110) surface and thus may have a shorter path length. The shorter diffusion path length gives rise to a smaller capture zone of oxygen and creates a higher number density of oxide nuclei. This is confirmed by our results in which the active zone of oxygen capture around each island on the Cu(110) surface is 0.3331 μm, which is significantly smaller than that on the Cu(100) surface (1.09 μm), as shown in Table I.

It has been reported that the O-chemisorption on the Cu(111) surface causes a disordered surface overlayer at room temperature, in which oxygen atoms have more than one well-defined height with respect to the Cu surface.[21] As the temperature increases to 200–350 °C, the chemisorption of oxygen on the Cu(111) surface results in ordered "29," ($\sqrt{13}$ $R46.1° \times 7R21.8°$), and "44," ($\sqrt{73}R5.8° \times \sqrt{21}R - 10.9°$), lattice structures, as shown in Fig. 9(c).[22–26] These structures comprise distorted hexagonal arrays of O atoms arranged in parallel lines in the first layer, with the unit cell areas 29 and 44 times larger than that of the substrate Cu(111), which appears strikingly similar to the (111)$Cu_2O$ structure. Both chemisorbed oxygen layers are considered to be analogous to the planes of the $Cu_2O$(111) surface that has a structure with equilateral hexagons of oxygen atoms in the first layer. Therefore, the reconstructed Cu{111} surface is

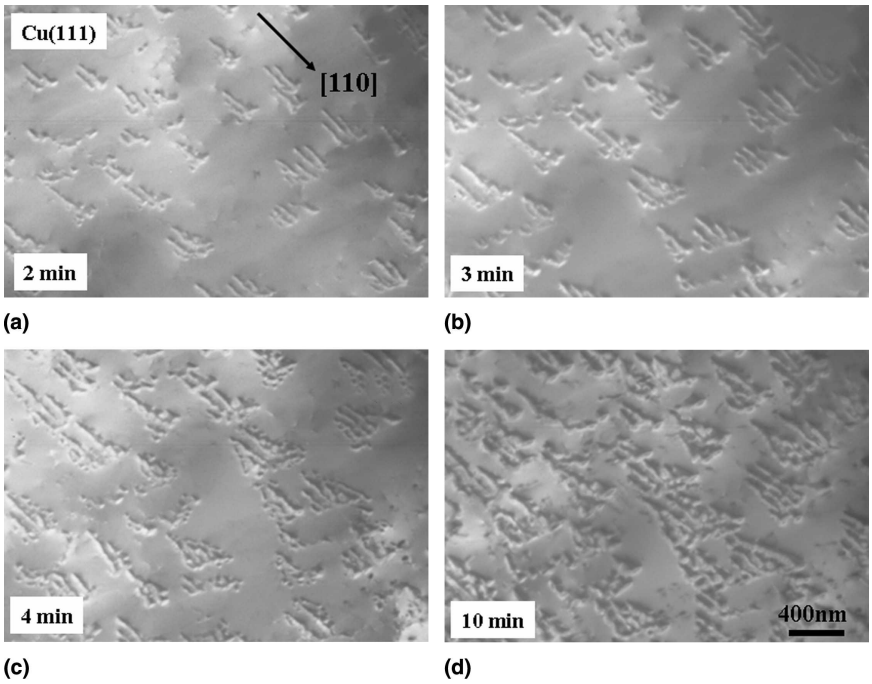


FIG. 7. In situ BF TEM sequence images taken as a function of oxidation time in the oxidation of Cu(111) thin film at 450 °C and an oxygen pressure of $5 \times 10^{-4}$ Torr.

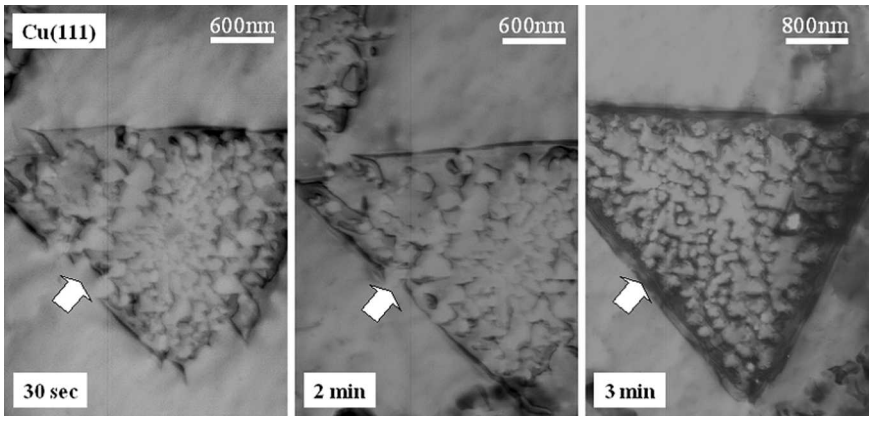


FIG. 8. In situ BF TEM sequence images taken as a function of oxidation time at a constant oxygen pressure of $5 \times 10^{-5}$ Torr and a temperature of 600 °C.

almost a template for the $Cu_2O$ {111} structure, which facilitates the nucleation of the $Cu_2O$ structure and gives rise to the fastest initial nucleation rate of the oxide islands.

### B. Effect of energetics on the oxide formation

To form oxide islands on the surface, the system should overcome an activation barrier the height of which is given by the work of formation of the critical nuclei. The number of critical nuclei per unit area is

$$N_{r^*} = N_0 \exp\left(-\frac{\Delta F^*}{kT}\right) \quad , \qquad (7)$$

where $r^*$ is the radius of the critical nucleus, $N_0$ is the number of nucleation sites per unit area of substrate surface, $\Delta F^*$ is the free energy of formation of the critical nucleus, and $k$ and $T$ have their usual meanings. The main contributions to $\Delta F^*$ are the unit volume of energy, the surface/interfacial energy, and the interfacial strain energy related to the lattice mismatch.

The unit volume energy is the same for the oxide islands formed on Cu(100) and (110) surfaces since only $Cu_2O$ is observed to form. The interfacial strain energy is a function of the Poisson ratio ($\nu$) and shear modulus ($\mu$) of the substrate, and oxide island bulk stress ($\sigma_b$).[27,28] The interfacial strain energies, due to lattice mismatch

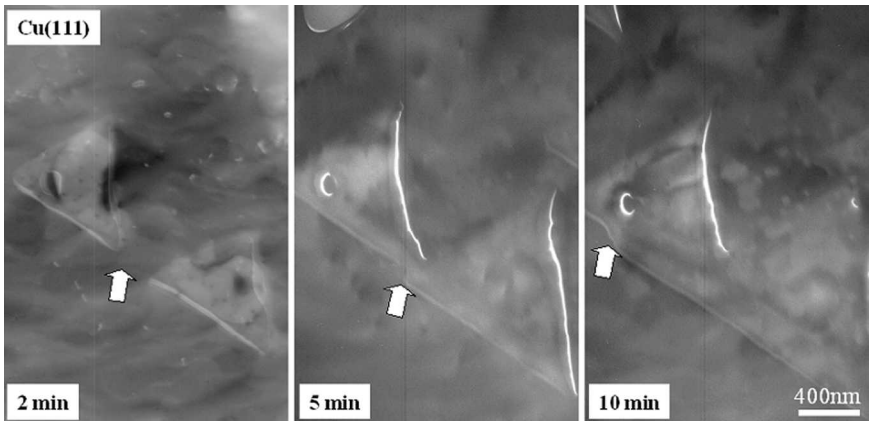


FIG. 9. In situ BF TEM sequence images of the 2D oxide growth as a function of oxidation time at 700 °C and a constant oxygen pressure of $5 \times 10^{-5}$ Torr.

and elastic relaxations, in oxide islands formed on both surfaces are similar because both form crystallographically aligned $Cu_2O$ islands. However, the difference in surface energies of Cu(110) and (100) should play an important role in the nucleation behavior. The surface energy of Cu(100) is 1280 mJ/m$^2$, which is lower than that for Cu(110) (1400 mJ/m$^2$).[29] Therefore, it is expected that the Cu(110) surface will be less stable and the nucleation of oxide islands will be facilitated. As a result, the Cu(110) surface has a smaller activation energy for the nucleation of the oxide islands and a higher nuclei density of oxide, as shown in Table I.

Our results regarding the formation of oxide islands at different oxidation temperatures indicate that the oxidation temperature has a dramatic effect on the interfacial strain between the oxide and the substrate, leading to the different morphologies and growth modes of the oxide islands in the oxidation of Cu(100) and Cu(110) surfaces. For example, oxide islands with different shapes (e.g., triangular, domed, elongated, or pyramidal) can be obtained by simply changing only the oxidation temperature in the oxidation of Cu(100).[27,30] The oxide islands formed in the oxidation of the Cu(110) surface have a trapezoid shape projected on the metal surface, as shown in Fig. 4(b). The change in the oxidation temperature does not change this trapezoid shape, but changes the thickness of the oxide islands (i.e., a deeper embedding of the islands into the substrate at higher temperatures).[16,17]

In comparison with the Cu(100) and (110) surfaces, the Cu(111) surface shows the different nucleation and growth behaviors of the oxide due to the perfect template of the O-chemisorbed layer for oxide formation. The Cu(111) surface exhibits the fastest nucleation rate for oxide islands for oxidation at temperatures lower than 550 °C compared with the Cu(100) and (110) surfaces. However, the oxidation of Cu(111) in the temperature range of 550–700 °C results in a very fast lateral growth of the oxide without an obvious nucleation of the island. A number of fundamental aspects of the growth of 3D islands in heteroepitaxy are now well-documented,[31–33] and it is typically believed that a misfit strain drives the formation of the 3D islands. The elastic energy of the initially planar, strained layer increases with growing film thickness until the system can lower its free energy by nucleating faceted 3D islands, thus relaxing part of the misfit strain at the expense of somewhat increased surface energy. Minimizing the total free energy of a strained island gives an activation energy barrier for the formation of a 3D island, and this barrier scales with lattice misfit $f$ as $f^4$.[34] Therefore, the lattice misfit plays a prominent role in determining the mode of growth. The larger the misfit, the greater the tendency toward island-like growth, and vice versa (i.e., layer-by-layer growth). On the other hand, the crystallographic orientation of the substrate also affects the mechanism of growth. The more densely packed the substrate plane, the greater the tendency toward layer-like growth in comparison with the less densely packed planes. $Cu_2O$ and Cu have thermal expansion coefficients of $1.9 \times 10^{-6}$ °C and $17 \times 10^{-6}$ °C, respectively. With increasing temperature, the lattice mismatch between Cu and $Cu_2O$ is reduced, and the O/Cu(111) surface forms an ideal template for the layer-by-layer growth of $Cu_2O$ without the "islanding" process at the high temperatures. In comparison with the Cu(100) and Cu(110) surfaces, the Cu(111) surface also provides a substrate with the most densely packed planes that facilitates the layer-by-layer growth of the oxide at high temperatures.

An important feature for Cu(111) surface oxidation is the formation of a discontinuous oxide layer in the temperature range of 550–650 °C. Earlier studies[22–26] demonstrated that the annealing of the O/Cu(111) surface at ~550 °C results in the conversion of disordered O/Cu(111) into ordered 29 and 44 surface structure domains. The formation of a discontinuous oxide layer on

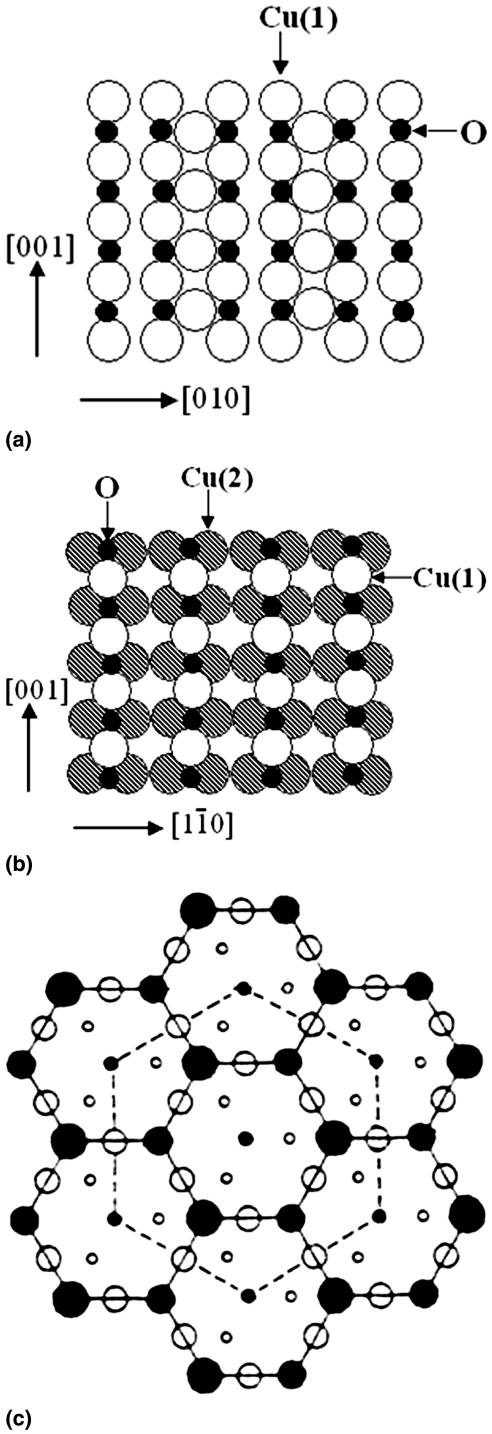


FIG. 10. Schematic diagram of the reconstructed (a), ($\sqrt{2} \times 2\sqrt{2}$)R45° O–Cu(100) surface (b), the (2 × 1)O–Cu(110) surface, and (c) the 29/44–Cu(111) surface due to oxygen chemisorption. Filled circles, O atoms; open circles, top-layer Cu atoms; shaded circles, second-layer Cu atoms.

the Cu(111) surface may be related to these ordered and disordered domain structures of O/Cu(111). We speculate that the regions having $Cu_2O$ oxide could have 29 or 44 ordered surface structures, whereas the discontinuous regions could be associated with the disordered surface structure. Further surface analysis is needed to confirm this.

The oxidation of Cu(111) at 700 °C results in the continuous oxide layer. Again, the formation of this continuous oxide layer may be related to the reduced misfit strain between $Cu_2O$ and the Cu(111) surface at 700 °C, which favors the 2D layer growth. The formation of the continuous oxide layer at 700 °C also suggests that the O/Cu(111) surface at this temperature may have a continuous and ordered structure that provides a perfect template for the 2D growth of the continuous oxide layer.

## VI. CONCLUSION

The initial oxidation stages of Cu(100), (110), and (111) surfaces have been investigated by in situ UHV TEM. It has been demonstrated that the surface structure and the strain between the oxide and copper substrate have a dramatic effect on the kinetics and energetics of oxide formation. The kinetic data on the nucleation and growth of $Cu_2O$ islands in the oxidation of Cu(100) and (110) surfaces indicate that Cu(110) shows a faster initial oxidation rate than Cu(100). The oxidation of the Cu(111) surface reveals a completely different behavior from that of the Cu(100) and (110) surfaces. The initial stages of Cu(111) oxidation are dominated by the nucleation of oxide islands at temperatures lower than 550 °C, and are dominated by the 2D growth of oxide layer at temperatures higher than 550 °C. This dependence of the oxidation kinetics on crystal orientation and temperature is attributed to the structures of the oxygen-chemisorbed layer, oxygen surface diffusion, surface energy, and the interfacial strain energy that underlie the oxide formation in the initial stages of metal oxidation.

## ACKNOWLEDGMENTS

This research project was funded by the National Science Foundation (Grant No. 9902863), Department of Energy—Basic Energy Science and a National Association of Corrosion Engineers seed grant. The experiments were performed at the Materials Research Laboratory, University of Illinois at Urbana-Champaign, which is supported by the U.S. Department of Energy (Grant No. DEFG02-96-ER45439). The authors kindly thank I. Petrov, R. Twesten, M. Marshall, and K. Colravy for their help.

## REFERENCES

1. C. Wagner: Beitrag zur theorie des anlaufvorgangs. *Z. Phys. Chem.* **B21,** 25 (1933).
2. N. Cabrera and N.F. Mott: Theory of the oxidation of metals. *Rep. Prog. Phys.* **12,** 163 (1948).
3. P.H. Holloway and J.B. Hudson: Kinetics of the reaction of oxy-

gen with clean nickel single crystal surfaces. *Surf. Sci.* **43,** 123 (1974).
4. W.H. Orr: Oxide nucleation and growth. Ph.D Thesis. Cornell University, Ithaca, NY, 1962.
5. J.C. Yang, M. Yeadon, B. Kolasa, and J.M. Gibson: Oxygen surface diffusion in three-dimensional $Cu_2O$ growth on Cu(001) thin films. *Appl. Phys. Lett.* **70,** 3522 (1997).
6. J.C. Yang, M. Yeadon, B. Kolasa, and J.M. Gibson: The homogeneous nucleation mechanism of $Cu_2O$ on Cu(001). *Scripta Mater.* **38,** 1237 (1998).
7. K. Thurmer, E. Williams, and J. Reutt-Robey: Autocatalytic oxidation of lead crystallite surfaces. *Science* **297,** 2033 (2002).
8. P. Marikar, M.B. Brodsky, C.H. Sowers, and N.J. Zaluzec: In situ HVTEM studies of the early stages of oxidation of nickel and nickel chromium-alloys. *Ultramicroscopy* **29,** 247 (1989).
9. J.M. Rakowski, G.H. Meier, and F.S. Pettit: The effect of surface preparation on the oxidation behavior of gamma TiAl-base intermetallic alloys. *Scripta Mater.* **35,** 1417 (1996).
10. J.C. Yang, B. Kolasa, J.M. Gibson, and M. Yeadon: Self-limiting oxidation of copper. *Appl. Phys. Lett.* **73,** 2841 (1998).
11. G.W. Zhou and J.C. Yang: Initial oxidation kinetics of copper (110) film investigated by in situ UHV-TEM. *Surf. Sci.* **531,** 359 (2003).
12. J.A. Venables, G.D.T. Spiller, and M. Hanbuecken: Nucleation and growth of thin films. *Rep. Prog. Phys.* **47,** 399 (1984).
13. M.L. McDonald, J.M. Gibson, and F.C. Unterwald: Design of an ultrahigh-vacuum specimen environment for high-resolution transmission electron microscopy. *Rev. Sci. Instrum.* **60,** 700 (1989).
14. G.W. Zhou and J.C. Yang: Reduction of $Cu_2O$ islands grown on a Cu(100) surface through vacuum annealing. *Phys. Rev. Lett.* **93,** 2261011 (2004).
15. S.M. Francis, F.M. Leibsle, S. Haq, N. Xiang, and M. Bowker: Methanol oxidation on Cu(110). *Surf. Sci.* **315,** 284 (1994).
16. G.W. Zhou and J.C. Yang: Temperature effects on the growth of oxide islands on Cu(110). *Appl. Surf. Sci.* **222,** 357 (2004).
17. G.W. Zhou and J.C. Yang: In situ UHV-TEM investigation of the kinetics of initial stages of oxidation on the roughened Cu(110) surface. *Surf. Sci.* **559,** 100 (2004).
18. K.W. Jacobsen and J.K. Norskov: Theory of the oxygen-induced restructuring of Cu(110) and Cu(100) surfaces. *Phys. Rev. Lett.* **65,** 1788 (1990).
19. F. Jensen, F. Besenbacher, E. Lagsgaard, and I. Stensgaard: Dynamics of oxygen-induced reconstruction of Cu(100) studied by scanning tunneling microscopy. *Phys. Rev. B* **42,** 9206 (1990).
20. I.K. Robinson, E. Vlieg, and S. Ferrer: Oxygen-induced missing-row reconstruction of Cu(001) and Cu(001)-vicinal surfaces. *Phys. Rev. B: Condens. Matter* **42,** 6954 (1990).
21. S.M. Johnston, A. Mulligan, V. Dhanak, and M. Kadodwala: The structure of disordered chemisorbed oxygen on Cu(111). *Surf. Sci.* **519,** 57 (2002).
22. F. Jensen, F. Besenbacher, E. Lagsgaard, and I. Stensgaard: Oxidation of Cu(111): Two new oxygen induced reconstructions. *Surf. Sci.* **259,** L774 (1991).
23. F. Jensen, F. Besenbacher, and I. Stensgaard: Two new oxygen induced reconstruction on Cu (111). *Surf. Sci.* **269/270,** 400 (1992).
24. F. Besenbacher and J.K. Norskov: Oxygen chemisorption on metal surfaces: general trends for Cu, Ni and Ag. *Prog. Surf. Sci.* **44,** 5 (1993).
25. T. Matsumoto, R.A. Bennett, P. Stone, T. Yamada, K. Domen, and M. Bowker: Scanning tunneling microscopy studies of oxygen adsorption on Cu(111). *Surf. Sci.* **471,** 225 (2001).
26. S.M. Johnston, A. Mulligan, V. Dhanak, and M. Kadodwala: The structure of disordered chemisorbed oxygen on Cu (111). *Surf. Sci.* **519,** 57 (2002).
27. G.W. Zhou and J.C. Yang: Formation of quasi-one-dimensional $Cu_2O$ structures by in situ oxidation of Cu(100). *Phys. Rev. Lett.* **89,** 106101 (2002).
28. J. Tersoff and R.M. Tromp: Shape transition in growth of strained islands: Spontaneous formation of quantum wires. *Phys. Rev. Lett.* **70,** 2782 (1993).
29. S.M. Foiles, M.I. Baskes, and M.S. Daw: Embedded-atom-method functions for the fcc metals Cu, Ag, Au, Ni, Pd, Pt, and their alloys. *Phys. Rev. B* **33,** 7983 (1986).
30. G.W. Zhou and J.C. Yang: Temperature effect on the $Cu_2O$ oxide morphology created by oxidation of Cu(001) as investigated by in situ UHV TEM. *Appl. Surf. Sci.* **210,** 165 (2003).
31. F.M. Ross, J. Tersoff, and R.M. Tromp: Coarsening of self-assembled Ge quantum dots on Si(001). *Phys. Rev. Lett.* **80,** 984 (1998).
32. G. Mederros-Ribeiro, A.M. Bratkovski, T.I. Kamins, D.A.A. Ohlberg, and R.S. Williams: Shape transition of germanium nanocrystals on a silicon (001) surface from pyramids to domes. *Science* **279,** 3534 (1998).
33. J.A. Floro, E. Chason, R.D. Twesten, R.Q. Hwang, and L.B. Freund: SiGe coherent islanding and stress relaxation in the high mobility regime. *Phys. Rev. Lett.* **79,** 3946 (1997).
34. J. Tersoff and F.K. LeGoues: Competing relaxation mechanisms in strained layers. *Phys. Rev. Lett.* **72,** 3570 (1994).